Effects of Graphene Nanopetal Outgrowths on Internal Thermal Interface Resistance in Composites (Supporting Information)

S1. Graphene-petal growth over fiber tows

The SEM image in Figure S1(a) contains a low-magnification view of a several fibers in a tow of 6000 fibers. Growth on a tow requires higher plasma power (1000 W) and pressure (40 Torr). The fiber in Figure S1(b) without petals reveals the sensitivity of the growth to process parameters. In this case growth was attempted at a slightly higher power of 300 W (instead of 200 W) at 10 Torr on a single fiber, and only a uniform amorphous deposition occurred.

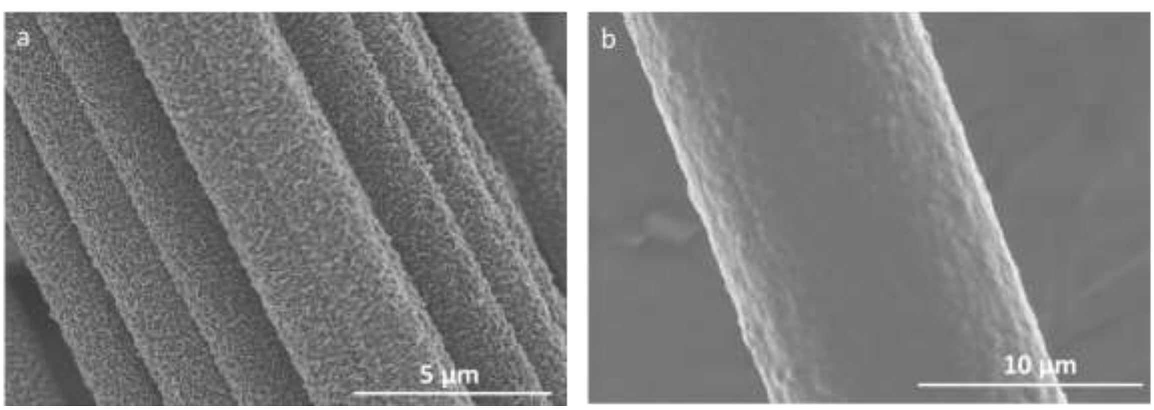

Figure S1. (a) Petal growth on a fiber tow (containing 6000 fibers) (b) A fiber without petals after processing at 300 W at 10 Torr showing sensitivity of the growth to process parameters.

We have found that the coupling of plasma to the fiber is crucial for obtaining graphene petal growth. Contrary to growth on carbon fiber tows where growth occurred at a pressure of 30 Torr and a plasma power of 700 W with 10 sccm of CH_4, we found best conditions for growth on a single fiber to occur at a pressure of 10 Torr and plasma power of 150 to 200 W with 10 sccm of CH_4 and 50 sccm of H_2. 700 W of plasma at 30 Torr was found to be too strong for a single fiber, as the portion of the fiber within the plasma would very often break. For fibers that could survive such conditions, only a thick amorphous deposition (Figure S1) around the fiber was observed.

S2. Sample preparation

In order to prepare samples for 3ω testing, a template for suspending the fibers was prepared. The template consisted of four parallel Cu wires wrapped around a circular Teflon ring. A single fiber was pulled out of a bundle of YSH 50 fibers. The fiber was then gently placed over the four Cu wires around the Teflon ring. In the 3ω experiment, the outer two wires are connected to a current source, while the middle two wires serve as voltage probe. In order to bond the fiber to Cu wires, a drop of electrically conductive Ag epoxy (H2OE Epotek two part Ag epoxy) was applied that was subsequently cured at 175 ^oC for 5 minutes. Figure S2 shows a Raman spectrum as obtained from a fiber tow. The spectrum indicates the crystalline and graphitic nature of the fiber with prominent peaks corresponding to the D band (~1350 cm^{-1}), G band (~1580 cm^{-1}) and 2D band (~ 2700 cm^{-1}) of graphite.

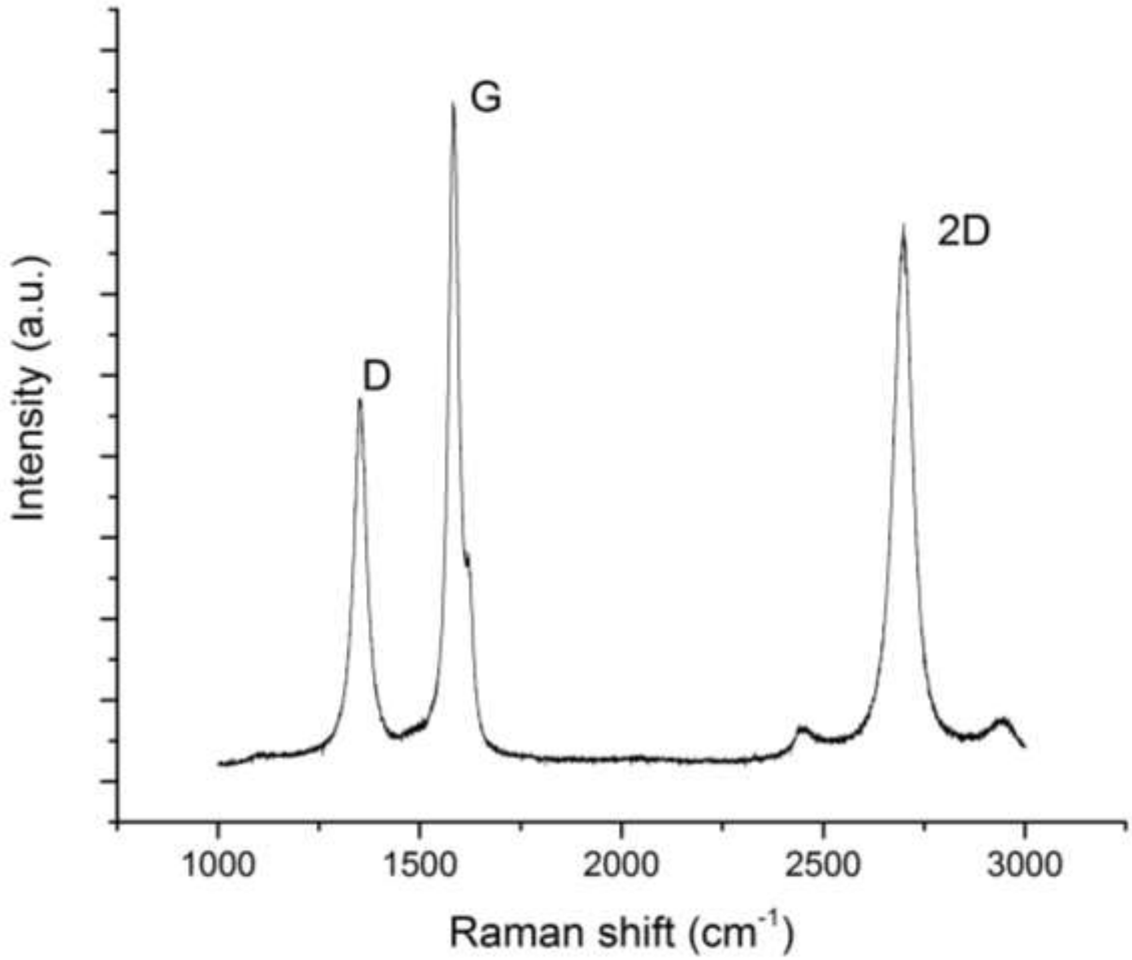

Figure S2. Raman spectrum as obtained from a fiber tow indicating graphitic nature of the carbon fiber.

An Epon 862/Epicure W epoxy (mixed in a ratio of 100:26 by weight) was used as matrix material for the composite. Epon 862 is a widely used epoxy in carbon fiber composites. The mixture was then gently poured into a container holding the suspended carbon fiber. Care was taken to not break the suspended fibers as they were submerged in the epoxy. The sample was then slowly heated to 120 ^{o}C over a period of 3 hours, after which it allowed to cool to room temperature. This was then followed by a post-bake at 175 ^{o}C for 3 hours.

A current source (Keithley, model 6221) was used to drive a sinusoidal current through the carbon fiber at the desired frequency. A lock-in amplifier (SR 850) was used to detect the 3ω voltage. 6 working samples, 3 each of bare fiber and petal-decorated fiber (out of a total of 50 prepared) could be obtained. Samples were lost at various stages of sample preparation where either the fiber or the fiber-Cu contact developed a discontinuity or a crack. The damage can be attributed to vibration induced during sample handling and/or to the viscous forces acting on the fiber due to flow of ambient air or epoxy around it.

S3. Derivation of the 3*ω* voltage

Here, we provide a brief theoretical development for extracting the 3*ω* voltage. For a fiber (radius '*a*') embedded in a matrix of infinite thickness, the Joule heat produced by a sinusoidal current through the fiber would result in a periodic temperature rise of both fiber as well as the surrounding matrix. Let the temperature rise be given by $\theta_f(r,t)$ and $\theta_m(r,t)$ for the fiber and the matrix respectively. Also, the sensitivity of electrical resistance (R) of fiber to temperature is given by β. Thus,

$$\beta = \frac{dR}{dT} \tag{1}$$

The governing equation for the steady-periodic temperature rise $\theta_m(r,t)$ in the matrix surrounding the fiber is

$$\frac{\partial^2 \theta_m(r,t)}{\partial r^2} + \frac{1}{r}\frac{\partial \theta_m(r,t)}{\partial r} = \frac{1}{\alpha_m}\frac{\partial \theta_m(r,t)}{\partial t} \tag{2}$$

Here, $\theta_m=\theta_m(r,t)$ is the periodic temperature rise in the matrix due to Joule heating at 2ω frequency, and α_m is the thermal diffusivity of the matrix. $\theta_m(r,t)$ can be expressed as product of time independent function $\hat{\theta}_m$ and exponential function $exp(i2\omega t)$. Thus,

$$\theta_m(r,t) = \hat{\theta}_m . \exp(i2\omega t) \tag{3}$$

Substituting for $\theta_m(r,t)$ in Eq. 2 results in a time-independent governing equation

$$\frac{\partial^2 \hat{\theta}_m}{\partial r^2} + \frac{1}{r}\frac{\partial \hat{\theta}_m}{\partial r} = q_m^2 \hat{\theta}_m \tag{4}$$

The complex quantity q_m is given by

$$q_m = \sqrt{\frac{i2\omega}{\alpha_m}} \tag{5}$$

The first boundary condition is obtained by conserving energy at the interface

$$-k_m(2\pi a l)\left.\frac{\partial \hat{\theta}_m}{\partial r}\right|_{r=a} = I^2 R \tag{6}$$

where k_m is the thermal conductivity of matrix. A condition of zero temperature rise far away from the heater provides the second boundary condition

$$\left.\hat{\theta}_m\right|_{r\to\infty} = 0 \tag{7}$$

The solution to Eq. 4 is,

$$\hat{\theta}_m = \varepsilon_1 I_0(q_m r) + \varepsilon_2 K_0(q_m r) \tag{8}$$

where I_0 and K_0 are modified Bessel functions of the first and second kind respectively.

The magnitude of q_m^{-1} represents the thermal penetration depth. Applying the boundary condition of Eq. 7, we find the requirement, $\varepsilon_1=0$. Thus, the solution to Eq. 4 is of the form $\hat{\theta}_m=\varepsilon_2 K_0(q_m r)$

Applying Eq. 6, one obtains,

$$\varepsilon_2 = \frac{I^2 R}{2\pi a l(k_m q_m K_1)} \tag{9}$$

Thus, the reduced solution for temperature in the matrix is

$$\hat{\theta}_m = \frac{I^2 R}{2\pi a l}\left(\frac{K_0(q_m r)}{K_1(q_m a)}\right) \tag{10}$$

For a line heater (a = 0), the solution further reduces to

$$\hat{\theta}_m = \frac{I^2 R}{2\pi k_m l} K_0(q_m r) \tag{11}$$

The third harmonic voltage ($V_{3\omega}$) is the product of the driving current (I) and the fluctuation in electrical resistance ($\hat{\theta}_f \cdot \frac{dR}{dT}$). Thus,

$$V_{3\omega} = \hat{\theta}_f \frac{dR}{dT} I \tag{12}$$

Assuming no resistance at the interface (i.e., $\hat{\theta}_m = \hat{\theta}_f$), and substituting for $\hat{\theta}_m$ from Eq. 10 into Eq. 12 we obtain,

$$V_{3\omega} = \frac{I^3 R\left(dR/dT\right)}{2\pi a l}\left(\frac{K_0\left(q_m r\right)}{k_m q_m K_1\left(q_m a\right)}\right) \tag{13}$$

which highlights the important proportionality between voltage and current,

$$V_{3\omega} \propto I^3 \tag{14}$$

If we consider an interfacial thermal resistance R_i'' between the heated element (carbon fiber in this case) and the surrounding matrix (epoxy), then the boundary condition in Eq. 5 is modified to

$$\left(\hat{\theta}_f - \hat{\theta}_m\right)_{r=a} = R_i''\left(\frac{I^2 R}{2\pi a l}\right) \tag{15}$$

which is an expression for the temperature jump at the interface. Substituting for $\hat{\theta}_m$ (Eq. 10) we obtain,

$$\hat{\theta}_f = \frac{I^2 R}{2\pi a l}\left(\frac{K_0(q_m a)}{k_m q_m K_1(q_m a)} + R_i^{''}\right) \tag{16}$$

Thus, an interface resistance ($R_i^{''}$) causes a frequency-independent constant shift in the in-phase component of the temperature fluctuation.

In the low-frequency regime, the out-of-phase part has a linear profile, the slope of which can be shown to be sensitive to the thermal conductivity (k_m) of the matrix/susbtrate. A fit to the initial linear regime is often used to obtain substrate thermal conductivity using the 3ω method. Interfacial resistance results in a constant upward shift in the in-phase component while the out-of-phase component remains unaffected.

The analysis thus far ignored the physical properties of the heater/fiber (e.g., specific heat, density, thermal conductivity) were ignored. This can be justified in the low frequency regime when the penetration depth is much larger than fiber diameter. The penetration depth (λ) of the thermal wave in the matrix is given by,

$$\lambda = \sqrt{\frac{\alpha_m}{2\omega}} \tag{17}$$

where α_m is the thermal diffusivity of matrix and ω the frequency of sinusoidal current. In the frequency regime where penetration depth is comparable to the fiber diameter, the effect of fiber/heater properties can no longer be neglected.

The governing equation for radial heat diffusion within the fiber is given by

$$\frac{\partial^2 \theta_f(r,t)}{\partial r^2} + \frac{1}{r}\frac{\partial \theta_f(r,t)}{\partial r} + \frac{q^{'''}}{k_f} = \frac{1}{\alpha_f}\frac{\partial \theta_f(r,t)}{\partial t}, r \le a. \tag{18}$$

where $q^{'''} = \frac{I^2 R}{\pi a^2 l}$ is the heat generated per unit volume in the fiber.

Similarly, the governing equation for heat diffusion in the matrix is given by

$$\frac{\partial^2 \theta_m(r,t)}{\partial r^2} + \frac{1}{r}\frac{\partial \theta_m(r,t)}{\partial r} = \frac{1}{\alpha_m}\frac{\partial \theta_m(r,t)}{\partial t}, \; r > a. \tag{19}$$

Substituting $\theta_f(r,t) = \hat{\theta}_f .\exp(i2\omega t).$ in Eq. 18 results in

$$\frac{\partial^2 \hat{\theta}_f}{\partial r^2} + \frac{1}{r}\frac{\partial \hat{\theta}_f}{\partial r} + \frac{q'''}{k} = q_f^2 \hat{\theta}_f \;, \; r \le a \tag{20}$$

Equation 20 is a non-homogeneous second order differential equation, the solution for which can be obtained by combining the solution for the corresponding homogeneous equation with a particular solution of the non-homogeneous equation. Finite temperature at $r = 0$ leads to

$$\hat{\theta}_f = \eta I_0(q_f r) + \frac{q'''}{k_f q_f^2} \tag{21}$$

As discussed before for Eq. 2, the solution to Eq. 19 is of the form

$$\hat{\theta}_m = \varepsilon K_0(q_m r) \tag{22}$$

The two constants (η and ε) can be obtained using the two boundary conditions of constant heat flux at the interface and a temperature jump at the interface due to interface resistance R_i''. The temperature jump leads to

$$\eta I_0(q_f a) + \frac{q'''}{k_1 q_f^2} = \varepsilon K_0(q_m a) + q''' R_i'' \frac{a}{2} \tag{23}$$

Applying the condition of continuous heat flux across the interface one obtains

$$-\eta k_f q_f I_1(q_f a) = \varepsilon k_m q_m K_1(q_m a) \tag{24}$$

The combination of Eq. 23 and Eq. 24 results in

$$\eta = q''' \left[R_i'' \frac{a}{2} - \frac{1}{k_f q_f^2} \right] \left[I_0(q_f a) + k_f q_f I_1(q_f a). \frac{K_0(q_m a)}{k_m q_m K_1(q_m a)} \right]^{-1} \tag{25}$$

and

$$\varepsilon = -\frac{\eta k_f q_f I_1(q_f a)}{k_m q_m K_1(q_m a)} \tag{26}$$

Substituting η into Eq. 21 gives the temperature rise of the fiber. If properties of the fiber and epoxy are known, the experimentally measured temperature rise can be fitted to Eq. 21 to obtain both thermal interface resistance ($R_i^{"}$) and matrix/epoxy thermal conductivity (k_m).

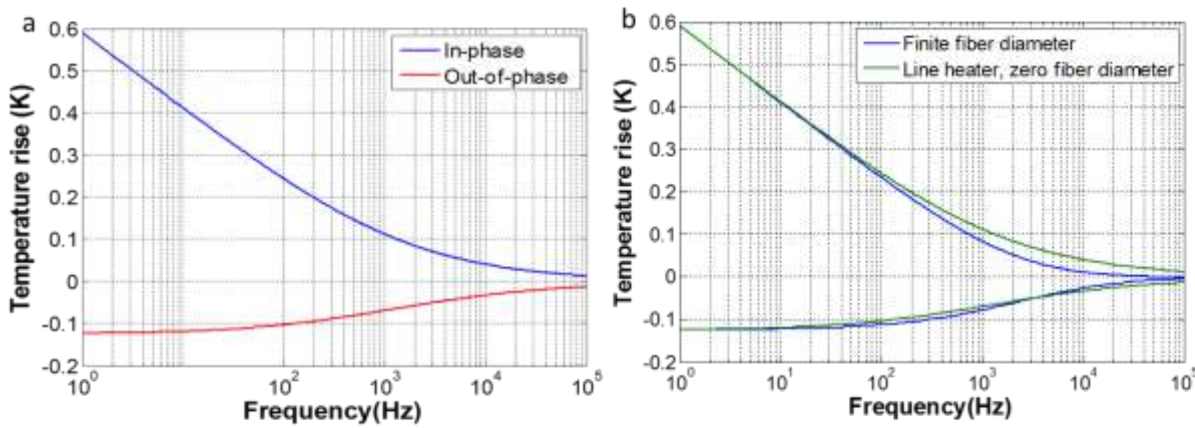

Figure S3. (a)Effect of interfacial resistance on in-phase and out-of-phase temperature rise in fiber. (b) Comparison of the idealized line heater case with the case for which physical properties of the heater/fiber are included. The effects of physical properties of the heart/fiber are more pronounced at high frequencies when the heat wave is localized in the vicinity of the fiber.

Figure S4 shows the effect of specific heat of epoxy on the temperature rise. The specific heat of epoxy has a less pronounced effect on the temperature rise, and the in general is most significant in the low-frequency regime when the heat wave penetrates much deeper into the epoxy.

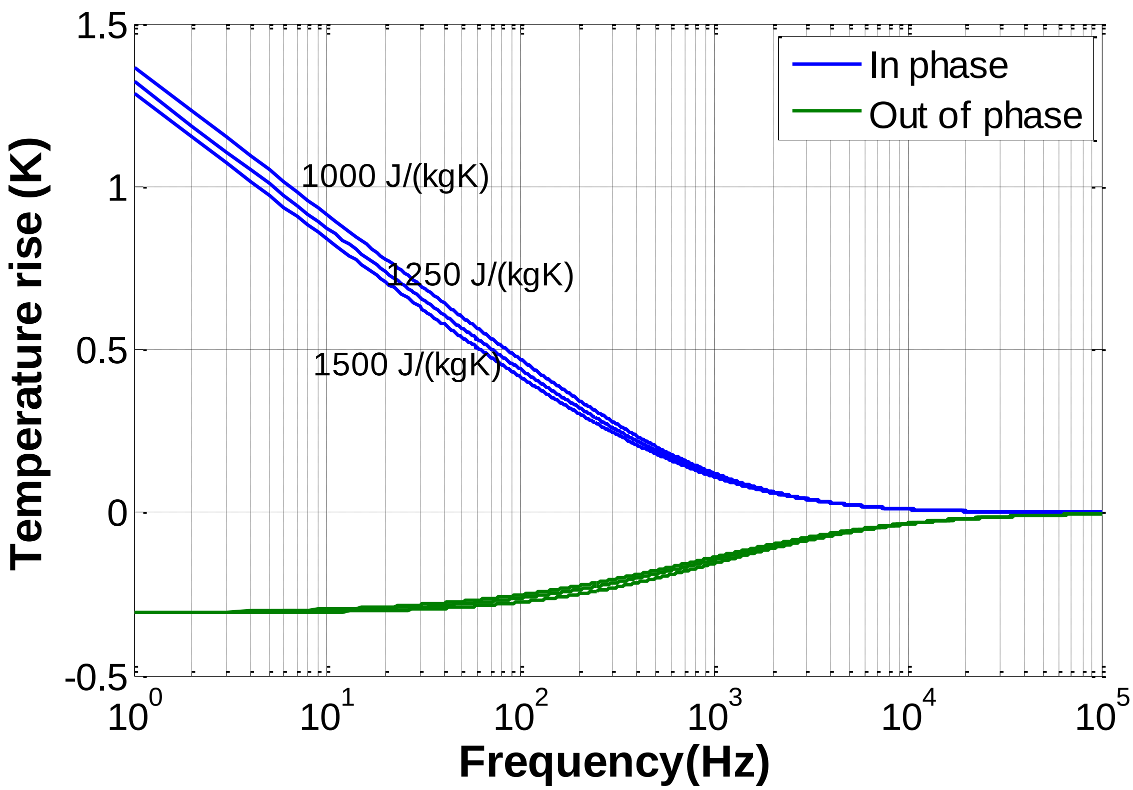

Figure S4. Effect of specific heat of epoxy on the temperature rise of fiber.

A fit to the experimental data was obtained using a nonlinear least-squares fitting algorithm. Interface resistance and epoxy thermal conductivity were set as two fitting parameters. The R-square goodness of fit for most samples had a value greater than 0.95, thereby indicating agreement between the model and the experimentally obtained data.

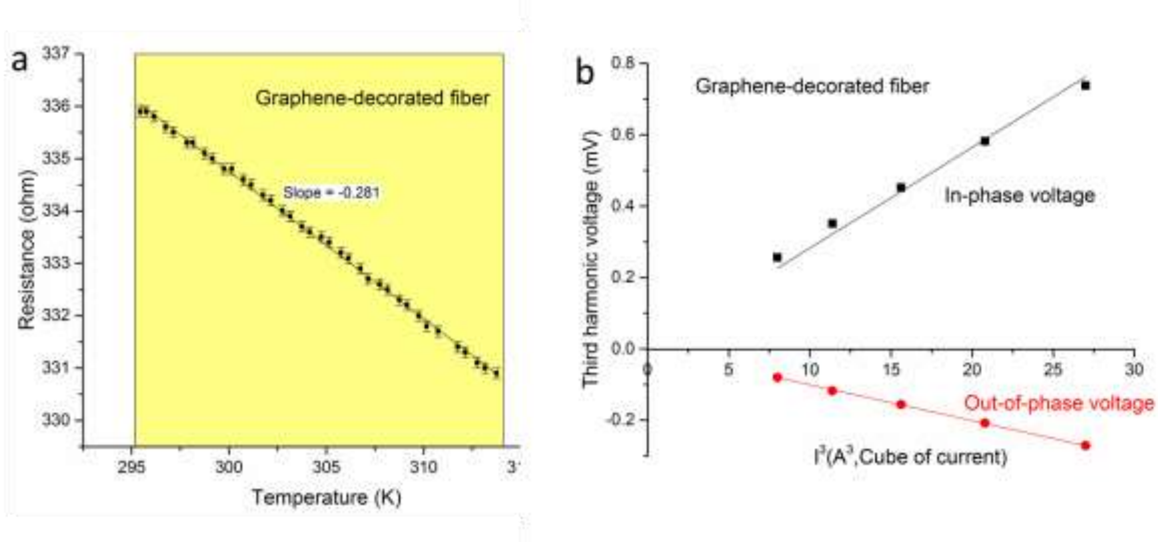

Figure S5. (a) Negative temperature coefficient of resistance for a graphene-decorated fiber (b) Cubic relationship between third harmonic voltage and driving current